Determination and theoretical analysis of supercritical fluid chromatographic retention of polycyclic aromatic hydrocarbons in a polymeric smectic phase

ARTICLE *in* THE JOURNAL OF PHYSICAL CHEMISTRY · APRIL 1992

Impact Factor: 2.78 · DOI: 10.1021/j100187a060

2 AUTHORS, INCLUDING:

Chao Yan
Shanghai Jiao Tong University
260 PUBLICATIONS **2,284** CITATIONS

Determination and Theoretical Analysis of Supercritical Fluid Chromatographic Retention of Polycyclic Aromatic Hydrocarbons in a Polymeric Smectic Phase

Chao Yan† and Daniel E. Martire*

Department of Chemistry, Georgetown University, Washington, D.C. 20057-2222
(Received: September 26, 1991)

A molecular theory of chromatography based on a mean-field lattice model has recently been developed to describe the partitioning of blocklike molecules between an isotropic mobile phase and an anisotropic stationary phase. A carefully designed capillary SFC experiment mimicking the theoretical model has been carried out. The retention behavior for PAH solutes with a smectic liquid-crystalline stationary phase and a supercritical fluid CO_2 mobile phase has been determined over a wide range of temperature and density. The theoretical predictions, such as the dependence of solute retention on the state variables (temperature and density) and molecular parameters (segmental interaction energies and molecular dimensions), are tested more quantitatively. In agreement with the theory, it is found that (a) the logarithm of the capacity factor k' (or the distribution coefficient K) is a linear function of the minimum area (A_{min}) of isomeric PAH solute molecules; (b) ln k' (or ln K) decreases with increasing mobile phase density (θ_m), more rapidly for solute molecules with a relatively larger contact area with the mobile phase; (c) ln k' (or ln K) increases linearly (in general) with increasing reciprocal temperature ($1/T$) and the slope of ln k' vs $1/T$ (van't Hoff plot) is more negative for solute molecules with a relatively larger ratio of contact area with the stationary phase to contact area with the mobile phase.

1. Introduction

An understanding of the molecular mechanism of solute retention is important because it not only facilitates informed selection of the right combination of mobile and stationary phase variables for a particular separation problem but also develops the potential of chromatography for physicochemical measurements by exploiting its equilibrium distribution process to obtain various properties involving the solute, mobile, and stationary phases.[1-4]

Liquid-crystalline stationary phases have shown unique selectivity for isomeric polycyclic aromatic hydrocarbon (PAH) compounds.[5] Immobilized bonded phases, such as (4,4'-dipentylbiphenyl)dimethylsiloxane (55B)[6] and octadecylsilane (C_{18})[7] polymeric phases, also exhibit excellent shape selectivity for isomeric PAHs that is similar to the shape selectivity observed for liquid-crystalline phases. In commonly used side-chain polymeric smectic stationary phases, the rodlike liquid-crystalline monomers bonded to flexible polysiloxane backbones are arranged in layers. An X-ray crystallography study has shown that within each layer, the long axes of the rodlike substituents are preferentially aligned in one direction to form a "brushlike" structure.[8] The "blocklike" PAH molecules penetrating into the stationary phase would prefer, both entropically and energetically, to align themselves with the stationary phase.[9]

In our preceding paper,[9] a molecular theory of chromatography, based on mean-field statistical thermodynamics, was developed to describe the partitioning of blocklike molecules between an isotropic mobile phase and an anisotropic stationary phase. The theory was qualitatively applied to the interpretation and analysis of experimental data in gas, liquid, and supercritical fluid chromatography (GC, LC, and SFC, respectively). However, most of the theoretical predictions remain to be further confirmed.

In the present study, a carefully designed capillary SFC experiment mimicking the theoretical model system has been carried out. The retention behavior for PAH (and polyphenyl) solutes with a smectic liquid-crystalline stationary phase and a supercritical fluid CO_2 mobile phase has been determined over a wide range of temperature and density. The effects of solute characteristics, mobile-phase parameters, stationary phase parameters, and temperature are examined more quantitatively. The theoretical findings are in general agreement with the experimental results.

2. Model and Retention Equation

In this section we will model our experimental system in order to calculate molecular dimensions and to test the theory. The details of the theory have been presented in our preceding paper.[9] Therefore, here we will only summarize the theoretical parts relevant to the analysis and discussion.

2.1. Model of Mobile Phase. The methodology for calculating the unit segmental volume (v_0 = 6.06 Å^3) of the lattice model system has been discussed in section 3.1 of the preceding paper.[9] We model a CO_2 molecule as a block with dimensions of qqr and a van der Waals volume of 32.72 Å^3/molecule. We assign a length-to-breadth ratio, r/q, of 1.83 based on the bond distance D(C=O) = 1.16 Å and the van der Waals radius of oxygen, 1.40 Å. The CO_2 dimensions relative to unit segmental length (l_0 = 1.82 Å) are q = 1.43 and r = 2.63, respectively.

The pure mobile phase, as a whole, is modeled as a system composed of these relatively small blocklike molecules isotropically distributed in the three-dimensional lattice.

The mobile-phase segmental number density or occupied volume fraction (θ_m) in our model can be related to the actual density of CO_2 (ρ_m) by $\theta_m = (v_0 L q^2 r \rho_m)/G \approx 0.45\rho_m$, where v_0 = 6.06 Å^3, L is Avogadro's number, and G is the molecular weight of CO_2.[9]

2.2. Model of Solutes. The solute molecules used in this study are 10 PAH compounds. (Although biphenyl and *p*-terphenyl are strictly not PAHs, for economy of presentation we shall refer to them as such.) A list of the solutes along with their relevant properties is provided in Table I. We model a PAH molecule as a block with dimensions of abc ($a \le b \le c$). According to X-ray crystallography, seven of the solutes are basically planar molecules.

† Present address: Analytical Research and Development, Building 360/1034, Sandoz Pharma Ltd., CH-4002 Basel, Switzerland.
* Corresponding author.

(1) Shim, J. J.; Johnston, K. P. *J. Phys. Chem.* **1991**, *95*, 353.
(2) Roth, M. *J. Phys. Chem.* **1990**, *94*, 4309.
(3) Dorsey, J. G.; Dill, K. A. *Chem. Rev.* **1989**, *89*, 331.
(4) Martire, D. E.; Boehm, R. E. *J. Phys. Chem.* **1983**, *87*, 1045.
(5) Witkiewicz, Z.; Mazur, J. *LC-GC* **1990**, *8*, 224.
(6) Lochmüller, C. H.; Hunnicutt, M. L.; Mullaney, J. F. *J. Phys. Chem.* **1985**, *89*, 5770.
(7) Wise, S. A.; Sander, L. C.; Chang, H. C.; Markides, K. E.; Lee, M. L. *Chromatographia* **1988**, *25*, 473.
(8) Talrose, R. V.; Sinitzyn, V. V.; Shibaev, V. P.; Plate, N. A. *Mol. Cryst. Liq. Cryst.* **1982**, *80*, 211.
(9) Yan, C.; Martire, D. E. *J. Phys. Chem.*, preceding article in this issue.

0022-3654/92/2096-3505$03.00/0

TABLE I: Solutes

name	mol wt	chem formula	struct	planarity
chrysene	228.30	$C_{18}H_{12}$	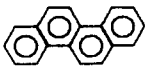	planar
benz[*a*]anthracene	228.30	$C_{18}H_{12}$	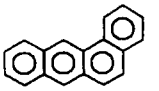	planar
triphenylene	228.30	$C_{18}H_{12}$	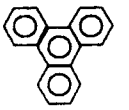	planar
benzo[*c*]phenanthrene	228.30	$C_{18}H_{12}$	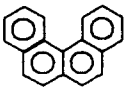	nonplanar
pyrene	202.26	$C_{16}H_{10}$	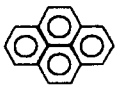	planar
anthracene	178.24	$C_{14}H_{10}$	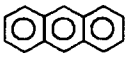	planar
phenanthrene	178.24	$C_{14}H_{10}$	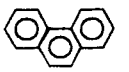	planar
naphthalene	128.18	$C_{10}H_8$	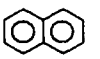	planar
p-terphenyl	230.31	$C_{16}H_{14}$	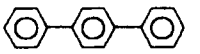	nonplanar
biphenyl	154.21	$C_{12}H_{10}$	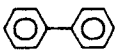	nonplanar

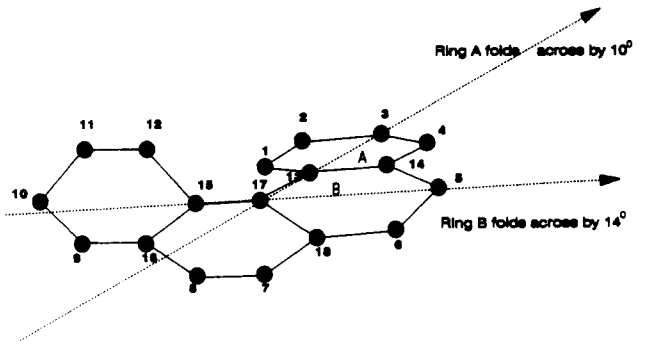

Figure 1. Perspective drawing of a molecule of benzo[*c*]phenanthrene.

However, repulsions between overcrowded atoms lead to deviations from planarity in three of them.[10-12] They are benzo[*c*]-phenanthrene, biphenyl, and *p*-terphenyl. A perspective drawing for benzo[*c*]phenanthrene is shown in Figure 1. The distance of 3.0 Å between the overcrowded atoms 1 and 12 is achieved by distortion of benzene rings from planarity. Ring B folds across the diagonal 5–17 by about 14° and ring A folds across the diagonal 3–13 by about 10°. This puts atoms 1 and 12 about 0.4 Å on opposite sides of a reference plane through 13, 15, 17, 18. *p*-Terphenyl and biphenyl in the solid state have interplane angles, on average, of 21° and 29°, respectively. The calculation of molecular dimensions was given in section 3.1 of the preceding paper.[9] The geometric parameters of the solutes are listed in Table II.

2.3. Model of Stationary Phase. The stationary phase used in this study is smectic biphenyl carboxylate ester polysiloxane. The structure of two units of the polymer is shown in Figure 2.

We cut a single unit off the polymer and model it as a rigid block with a square cross section ω^2 and length l. Furthermore, we assume that it has approximately the same cross-sectional area as does biphenyl ($\omega^2 = 4.84$, interplane angle 29°). The pure stationary phase (smectic), as a whole, is modeled as a system composed of these blocklike molecules arranged in layers; within each layer the molecules are assumed to be perfectly aligned in the (preferred) z direction.

A single unit of the polymer has a van der Waals volume of 400 Å^3 and a molecular weight G, of 420 g/mol. Thus, its segmental number should be $m = 400/v_0 = 66.01$ segments/molecule, where $v_0 = 6.06$ Å^3. The segmental number density or occupied volume fraction can be calculated:

$$\theta_s = (\rho_s v_0 L m)/G = (1.10 \times 6.06 \times 10^{-24} \times 6.02 \times 10^{23} \times 66.01)/420 = 0.63$$

segments/cell, where L is Avogadro's number, and ρ_s is the density in g/mL provided by Lee Scientific Inc. (the supplier).

2.4. Retention Equation (Distribution Coefficient). With $\alpha \rightarrow {}^1/_2$ and $\beta = \gamma \rightarrow 0$, eq 62 in ref 9 gives the retention equation for blocklike solutes fully aligned with the anisotropic stationary phase:

$$\ln (3K) = ab \ln\left[\frac{1-\theta_s}{1-\theta_s(1-1/\omega)}\right] - abc \ln\left[\frac{1-\theta_m}{1-\theta_m\left(1-\frac{2}{3q}-\frac{1}{3r}\right)}\right] - \left[\frac{2(ac+bc)\epsilon_{st}}{kT}\right]\left[\frac{\theta_s(1/\omega)}{1-\theta_s(1-1/\omega)}\right] + \left[\frac{2(ab+ac+bc)\epsilon_{mt}}{kT}\right]\left[\frac{\theta_m\left(\frac{2}{3q}+\frac{1}{3r}\right)}{1-\theta_m\left(1-\frac{2}{3q}-\frac{1}{3r}\right)}\right] \quad (1)$$

where θ_i and ϵ_{ij} are, respectively, the occupied volume fraction

(10) Herbstein, F. H.; Schmidt, G. M. J. *J. Chem. Soc.* **1954**, 3302.
(11) Charbonneau, G. P.; Delugeard, Y. *Acta Crystallogr.* **1977**, *B33*, 1586.
(12) Baudour, P. L.; Cailleau, Y. D. H. *Acta Crystallogr.* **1976**, *B32*, 150.

TABLE II: Geometric Parameters of Solutes[a]

solute	V_W', Å^3	dimensions, Å			rel parameters		
		a	b	c	A_{min}	A_{ef}	V_W
chrysene	207.77	2.57	6.66	12.13	5.16	38.90	34.29
benz[a]anthracene	207.77	2.57	7.38	10.95	5.71	38.54	34.29
triphenylene	207.77	2.57	8.53	9.48	6.60	38.29	34.29
benzo[c]phenanthrene	207.77	3.57	6.54	8.90	7.03	37.65	34.29
pyrene	181.01	2.57	7.38	9.54	5.71	34.31	29.87
anthracene	165.27	2.57	6.09	10.55	4.72	32.26	27.27
phenanthrene	165.27	2.57	6.51	9.88	5.04	32.06	27.27
naphthalene	122.77	2.57	5.97	8.01	4.62	25.21	20.26
p-terphenyl	218.79	3.35	4.76	13.74	4.80	38.33	36.10
biphenyl	149.45	3.65	4.47	9.15	4.92	27.31	24.66

[a] V_W' is the van der Waals volume in Å^3, and $V_W = V_W'/v_0$, $A_{min} = ab/a_0$ and $A_{ef} = (ab + ac + bc)/a_0$, where $v_0 = 6.06$ Å^3 and $a_0 = 3.32$ Å^2.

TABLE III: Natural Logarithm of Capacity Factor (ln k') of PAHs with SB-Smectic Column

	density, g/mL									
	0.15	0.20	0.25	0.30	0.35	0.40	0.45	0.50	0.55	0.60
					Temperature = 107 °C					
naphthalene	−1.17	−1.71	−2.30	−2.66	−3.00					
biphenyl	−0.46	−1.11	−1.71	−2.30	−2.81					
phenanthrene		1.17	0.46	−0.22	−0.78	−1.17	−1.66	−2.21		
anthracene		1.83	1.11	0.43	−0.12	−0.58	−1.05	−1.51		
pyrene			1.67	0.94	0.39	−0.11	−0.65	−1.14		
benzo[c]phenanthrene				1.42	0.76	0.18	−0.42	−0.97	−1.47	
triphenylene				1.87	1.18	0.58	−0.02	−0.56	−0.99	−1.43
p-terphenyl				2.31	1.64	1.04	0.43	−0.12	−0.54	−0.95
benz[a]anthracene					2.16	1.56	0.95	0.40	−0.05	−0.49
chrysene					2.71	2.11	1.53	0.97	0.54	0.08
					Temperature = 117 °C					
naphthalene	−1.14	−1.77	−2.21	−2.53						
biphenyl	−0.49	−1.17	−1.77	−2.21						
phenanthrene	1.81	1.09	0.44	−0.16	−0.73	−1.27	−1.61	−2.04		
anthracene		1.69	1.03	0.43	−0.11	−0.65	−1.08	−1.47		
pyrene			1.65	0.98	0.41	−0.13	−0.63	−1.08	−1.43	−1.90
benzo[c]phenanthrene			2.12	1.40	0.74	0.10	−0.42	−0.89	−1.31	−1.66
triphenylene				1.83	1.17	0.52	−0.01	−0.51	−0.94	−1.24
p-terphenyl				2.09	1.42	0.77	0.23	−0.26	−0.71	−1.02
benz[a]anthracene				2.79	2.11	1.47	0.92	0.41	−0.04	−0.37
chrysene					2.64	2.00	1.44	1.00	0.48	0.15
					Temperature = 127 °C					
naphthalene	−1.27	−1.83	−2.30	−2.66						
biphenyl	−0.65	−1.27	−1.83	−2.30	−2.66					
phenanthrene	1.66	0.95	0.30	−0.24	−0.78	−1.24	−1.71	−2.04		
anthracene	2.26	1.52	0.87	0.28	−0.26	−0.71	−1.17	−1.47	−1.83	
pyrene		2.25	1.53	0.90	0.31	−0.20	−0.67	−1.05	−1.47	
benzo[c]phenanthrene		2.75	1.99	1.28	0.64	0.07	−0.46	−0.89	−1.31	
triphenylene			2.44	1.71	1.05	0.47	−0.06	−0.51	−0.97	
p-terphenyl				1.83	1.16	0.57	0.02	−0.43	−0.89	
benz[a]anthracene				2.63	1.95	1.35	0.81	0.35	−0.12	
chrysene					2.45	1.85	1.30	0.83	0.37	
					Temperature = 137 °C					
naphthalene	−1.47	−1.90	−2.41							
biphenyl	−0.84	−1.39	−1.90	−2.41						
phenanthrene	1.44	0.76	0.13	−0.42	−0.89	−1.35	−1.77			
anthracene	1.98	1.29	0.65	0.09	−0.40	−0.84	−1.27	−1.61		
pyrene		2.05	1.35	0.74	0.20	−0.30	−0.76	−1.14	−1.56	
benzo[c]phenanthrane		2.58	1.80	1.11	0.52	−0.04	−0.54	−0.97	−1.43	
triphenylene			2.23	1.53	0.90	0.34	−0.17	−0.62	−1.11	
p-terphenyl			2.22	1.51	0.88	0.31	−0.21	−0.65	−1.11	
benz[a]anthracene				2.37	1.74	1.16	0.64	0.17	−0.24	
chrysene					2.20	1.62	1.10	0.63	0.20	
					Temperature = 147 °C					
naphthalene	−1.61	−2.04	−2.53							
biphenyl	−1.02	−1.56	−2.04	−2.41						
phenanthrene	1.21	0.56	−0.03	−0.54	−1.05	−1.51	−1.77			
anthracene	1.71	1.04	0.44	−0.09	−0.58	−1.05	−1.39	−1.77		
pyrene		1.83	1.17	0.59	0.05	−0.43	−0.87	−1.24		
benzo[c]phenanthrene		2.34	1.60	0.95	0.36	−0.17	−0.63	−1.08		
triphenylene			2.02	1.35	0.74	0.20	−0.29	−0.76		
p-terphenyl			1.89	1.21	0.59	0.04	−0.45	−0.92		
benz[a]anthracene				2.12	1.50	0.94	0.44	−0.02		
chrysene					1.93	1.38	0.86	0.40		

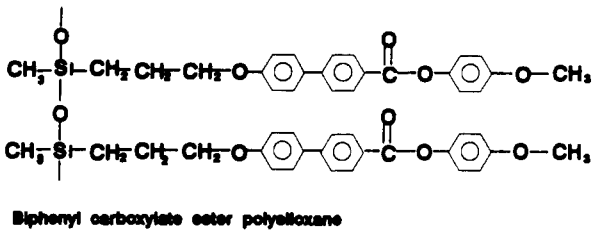

Figure 2. Structure of the stationary phase.

and (attractive) intermolecular interaction energy between immediately adjacent segments i and j. The subscripts s and m denote the stationary and mobile phases, respectively.

3. Experimental Section

3.1. Experimental Procedure. The chromatographic system consisted of a Model 501 Capillary Column Supercritical Fluid Chromatograph (Lee Scientific, Inc.; Salt Lake City, UT) which is controlled by a computer (Model 45945A, Hewlett-Packard, Sunnyvale, CA). The syringe pump assembly has a capacity of 175 mL and is surrounded by a cooling jacket attached to a refrigerated circulating bath. The water temperature was maintained at 10 °C during the filling process.

Injections were performed by a pneumatically operated injection valve (Valco Instrument Co., Inc.; Houston, TX) with a 200-μL sample loop. A 35 cm length of 10-μm-i.d. fused silica was used to split the sample upon injection. The split ratio was approximately 20:1, and the injection duration time was set at 0.01 s. A flame ionization detector (FID) was used for all experiments. The detector temperature was set at 325 °C. A chart recorder (Model 555, Linear Instruments Corp., Irvine, CA) was used to record the chromatograms. The mobile phase used was SFC grade carbon dioxide (Matheson Gas Products; Baltimore, MD).

The capillary column (SB–smectic phase) containing smectic liquid-crystalline polysiloxane (Figure 2) was 10 m long with a 50-μm i.d. and a film thickness of 0.15 μm. It has been reported that the stationary phase possesses a glassy-to-smectic transition point at about 100 °C and a smectic-to-isotropic transition point at about 300 °C.[13]

The solutes used were 10 PAHs (Aldrich Co., Inc.; Milwaukee, WI). They are differentiated by their retention order in the liquid-crystalline column as follows: naphthalene, biphenyl, phenanthrene, anthracene, pyrene, benzo[c]phenanthrene, triphenylene, p-terphenyl, benz[a]anthracene, and chrysene. Methylene chloride was used as the solvent (Fisher Scientific Inc.; NJ). Methane was injected as an "unretained" marker solute for determination of column void time (or hold-up time), t_0. It was found that the values of t_0 obtained from this method were in good agreement with those determined by a linearization of retention data for homologous series.[14] The concentration of each solute was approximately 2 mg/mL. The sample was injected and split by an approximate ratio of 20:1. It was determined that the solute concentration is well within the Henry's law region, i.e., "infinite dilution".

The experiments consisted of performing triplicate injections of the solutes for each temperature–density combination. Five temperatures were chosen at 10 °C intervals from 107 to 147 °C. For each temperature, injections were made at 0.05 g/mL density intervals from 0.15 to 0.60 g/mL. Each setting point was determined by fixing the pressure at a given temperature to give the desired density, which was determined using a modification of the BWR equation of state.[15] Since the pressure drop across the capillary column and its effect on solute retention are essentially negligible when the state of the SF mobile phase is far from the critical point,[15] we assumed that $\rho_{inlet} \approx \langle\rho\rangle \approx \rho$. Some solutes were excluded when experiments were run at each temperature–density combination. The inclusion and exclusion of any solute at a particular setting point were judged by its retention time (some are too short, some are too long). The retention time was obtained from the average value of the retention distances measured on the chart paper or the retention time read from the computer clock for three chromatograms of the solutes.

3.2. Results. The extensive capacity factor, k', is related to the intensive distribution coefficient as $K = k'(V_m/V_s)$, where V_m and V_s are the total volumes of the mobile and stationary phases, respectively. The capacity factor, k', was obtained from $k' = (t_R - t_0)/t_0$, where t_R is the retention time of the solute and t_0 is the column void time. The values of the natural logarithm of the capacity factor, ln k', of the solutes are tabulated in Table III.

4. Test of Theory and Discussion

Retention eq 1 is applicable to a system composed of blocklike solutes, an anisotropic stationary phase and an isotropic mobile phase. Our experimental system was designed to mimic the theoretical model.

The separability of the stationary phase contribution (the first and the third terms, with subscript s) and the mobile phase one (the second and the last terms, with subscript m) is evident in eq 1. Each term has two kinds of variables, namely, state variables (temperature and density) and molecular variables or parameters (molecular dimensions and interaction energies). However, once the chromatographic system is chosen, all the molecular parameters (through which the "chemical effect" will be exerted) are virtually fixed. Therefore, the state variables (through which the "state effect" will be exerted) are the only operational ones to be controlled.

4.1. Effect of Solute Characteristics. Rearranging eq 1, we have

$$\ln (3K) = Q_1 A_{min} + Q_2 A_{ef} + Q_3 V_w \tag{2}$$

where $A_{min} = ab$ is the minimum area, $A_{ef} = ab + ac + bc$ is the effective contact area, and V_w is the van der Waals volume for a solute molecule, respectively, and

$$Q_1 = \ln\left[\frac{1-\theta_s}{1-\theta_s(1-1/\omega)}\right] + \frac{2\epsilon_{st}}{kT}\left[\frac{\theta_s(1/\omega)}{1-\theta_s(1-1/\omega)}\right] \tag{3}$$

$$Q_2 = \frac{\theta_m\left(\frac{2}{3q}+\frac{1}{3r}\right)2\epsilon_{mt}}{\left[1-\theta_m\left(1-\frac{2}{3q}-\frac{1}{3r}\right)\right]kT} - \frac{\theta_s(1/\omega)2\epsilon_{st}}{[1-\theta_s(1-1/\omega)]kT} \tag{4}$$

$$Q_3 = \ln\left[\frac{1-\theta_m}{1-\theta_m\left(1-\frac{2}{3q}-\frac{1}{3r}\right)}\right] \tag{5}$$

For a specific chromatographic system at fixed operating conditions, Q_1, Q_2, and Q_3 should all be constants if all solutes considered belong to the same "family" and have equivalent segmental interaction energies, ϵ_{st} and ϵ_{mt}.

Considering that the van der Waals volumes are the same and the effective contact areas are very close for PAH solutes with the same number of rings, such as the four-ring isomers used in our experimental study (see Table IV), we may assume that the sum of the second and third terms in eq 2 is essentially a constant. Then, eq 2 can be written as

$$\ln k' = Q_1 A_{min} + \text{constant} \tag{6}$$

where the constant $= Q_2 A_{ef} + Q_3 V_w - \ln 3\phi$. The apparent phase

(13) Chang, H. K.; Markides, K. E.; Bradshaw, J. S.; Lee, M. L. *J. Chromatogr.* **1988**, *26*, 280.
(14) Reister, R. L.; Yan, C.; Martire, D. E. *J. Chromatogr.* **1991**, *588*, 289.
(15) Martire, D. E.; Riester, R. L.; Bruno, T. J.; Hussam, A.; Poe, D. P. *J. Chromatogr.* **1991**, *545*, 135.

TABLE IV: Minimum Areas and Retention Data for Four-Ring PAH Isomers with SB-Smectic Column at Mobile Phase Density of 0.35 g/mL

solute	A_{min}	temp, °C	ln k'
chrysene	5.16	107	2.71
		117	2.64
		127	2.45
		137	2.20
		147	1.93
benz[*a*]anthracene	5.17	107	2.16
		117	2.11
		127	1.95
		137	1.74
		147	1.50
triphenylene	6.60	107	1.18
		117	1.17
		127	1.05
		137	0.90
		147	0.74
benzo[*c*]phenanthrene	7.03	107	0.76
		117	0.74
		127	0.64
		137	0.52
		147	0.36

ratio is $\phi = V_m/V_s = d/4d_f = 83.33$, where d is the inner column diameter and d_f is the stationary phase film thickness. Equation 6 predicts a linear relationship of ln k' versus the minimum area (scaled) for isomeric solutes. Note that the slope Q_1 is predicted to be always negative since $\epsilon_{st} < 0$ and $\theta_s \leq 1$. The absolute value of Q_1 should decrease as the temperature increases since Q_1 is a function of $1/T$.

Least-squares analysis of the results in Table IV, according to eq 6, yields linear correlation coefficients in excess of 0.999. Representative plots of ln k' vs A_{min} for four-ring PAH isomers at constant temperatures are shown in Figure 3. The excellent agreement between the theory and the experimental results is evident. Figure 4 shows the plots of ln k' vs A_{min} for four-ring PAH isomers at constant density but different temperatures. It demonstrates that the absolute value of the slopes indeed decreases with the increasing temperature as predicted by the theory.

Since retention (ln k') is a function of several geometric parameters of the solute molecules (viz., A_{min}, A_{ef}, V_w), molecular size (van der Waals volume or carbon number) or L/B (length-to-breadth) ratio *alone* cannot predict accurately the retention behavior for the anisotropic system, not even the retention order.[7]

4.2. Effect of Mobile Phase Parameters. Once the stationary phase is chosen, the sum of the first and the third terms in eq 1 will be a constant for a particular solute at constant temperature. Then, eq 1 becomes

$$\ln K = -abc \ln\left[\frac{1-\theta_m}{1-\theta_m\left(1-\frac{2}{3q}-\frac{1}{3r}\right)}\right] + \left[\frac{(ab+ac+bc)2\epsilon_{mt}}{kT}\right]\left[\frac{\theta_m\left(\frac{2}{3q}+\frac{1}{3r}\right)}{1-\theta_m\left(1-\frac{2}{3q}-\frac{1}{3r}\right)}\right] + \ln K^\circ \quad (7)$$

where ln K° = the first term in eq 1 + the third term − ln 3 is the stationary phase contribution when the mobile phase density approaches zero. Interestingly, eq 7 reveals that the plots of ln K vs mobile phase density should be parallel for different stationary phases under identical conditions. The first term in eq 7, arising from the configurational entropy of the solute in the mobile phase, leads to an increase in ln K (or ln k') with increasing mobile phase density (θ_m). The second, usually dominant term reflects the mobile phase–solute attractive interactions and leads to a decrease in ln K with increasing θ_m. It is clear, from the coefficient (slope) of the term, that the decrease in ln K with increasing θ_m will be more rapid under the following conditions: (a) stronger mobile phase–solute interactions (more negative ϵ_{mt}); (b) larger contact area of the solute with the mobile phase; (c) lower temperature. Equation 7 also reveals that the slope for a particular solute should become less negative with increasing temperature. Shown in

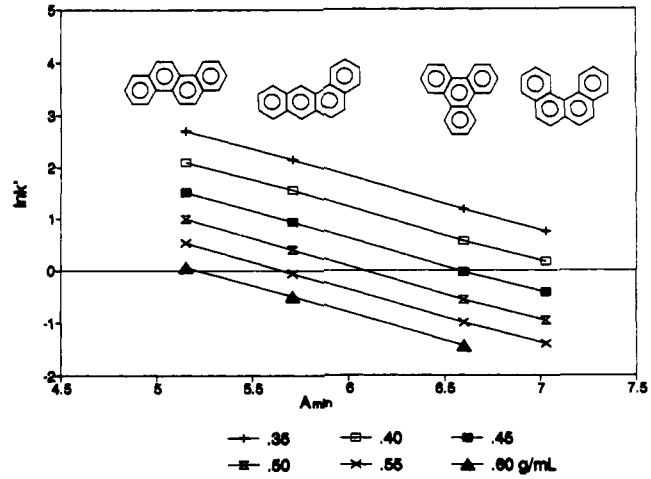

Figure 3. Linear dependence of ln k' on minimum area (scaled) of solute (A_{min}) for four-ring PAH isomers on the SB–smectic column at 107 °C and different mobile phase densities, as predicted by eq 6. Symbols: experimental data.

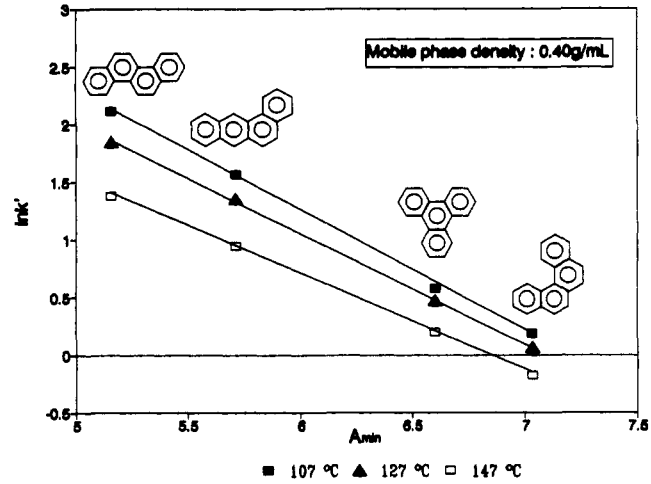

Figure 4. Linear dependence of ln k' on minimum area (scaled) of solute (A_{min}) for four-ring PAH isomers in the SB–smectic column at mobile phase (CO_2) density of 0.40 g/mL and different temperatures, as predicted by eq 6. Symbols: experimental data.

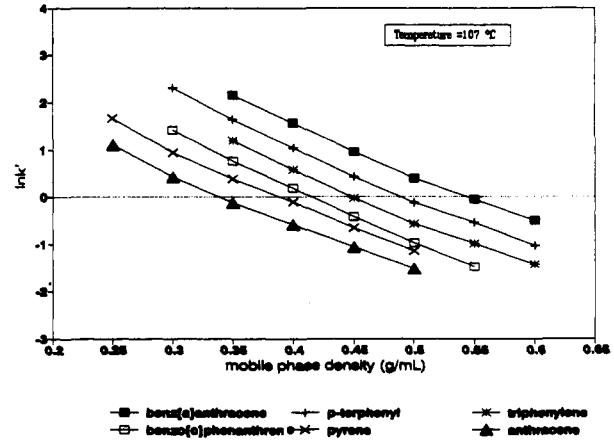

Figure 5. Plots of ln k' vs SF CO_2 mobile phase density for PAH solutes on the SB–smectic phase.

TABLE V: Experimental Data and Theoretical Results for Three PAH Isomers at 107 °C

	CO_2 density		retention data			CO_2 density		retention data	
solute	ρ_m, g/mL	θ_m,[a] seg/cell	ln k'(exp.)	ln k'(theor)[b]	solute	ρ_m, g/mL	θ_m,[a] seg/cell	ln k'(exp.)	ln k'(theor)[b]
triphenylene	0.25	0.11			benz[a]anthracene	0.90	0.40		-3.56
	0.30	0.13		1.61		0.95	0.43		-4.02
	0.35	0.16	1.19	1.09		1.00	0.45		-4.46
	0.40	0.18	0.58	0.57		1.05	0.47		-4.89
	0.45	0.20	-0.02	0.03		1.10	0.49		-5.29
	0.50	0.22	-0.56	-0.46		1.15	0.51		-5.66
	0.55	0.25	-0.99	-0.98		1.20	0.54		-6.00
	0.60	0.27	-1.43	-1.49		1.25	0.56		-6.30
	0.65	0.29		-2.00		1.30	0.58		-6.56
	0.70	0.31		-2.50		1.35	0.60		
	0.75	0.34		-3.00		1.40	0.63		
	0.80	0.36		-3.49		1.45	0.65		
	0.85	0.38		-3.97	chrysene	0.25	0.11		
	0.90	0.40		-4.43		0.30	0.13		3.24
	0.95	0.43		-4.89		0.35	0.16	2.71	2.70
	1.00	0.45		-5.32		0.40	0.18	2.11	2.17
	1.05	0.47		-5.74		0.45	0.20	1.53	1.60
	1.10	0.49		-6.13		0.50	0.22	1.05	1.10
	1.15	0.51		-6.49		0.55	0.25	0.54	0.56
	1.20	0.54		-6.82		0.60	0.27	0.07	0.03
	1.25	0.56		-7.11		0.65	0.29		-0.50
	1.30	0.58		-7.36		0.70	0.31		-1.02
	1.35	0.60				0.75	0.34		-1.54
	1.40	0.63				0.80	0.36		-2.05
	1.45	0.65				0.85	0.38		-2.55
benz[a]anthracene	0.25	0.11				0.90	0.40		-3.03
	0.30	0.13		2.58		0.95	0.43		-3.51
	0.35	0.16	2.16	2.06		1.00	0.45		-3.97
	0.40	0.18	1.56	1.53		1.05	0.47		-4.41
	0.45	0.20	0.95	0.98		1.10	0.49		-4.82
	0.50	0.22	0.40	0.48		1.15	0.51		-5.21
	0.55	0.25	-0.05	-0.04		1.20	0.54		-5.56
	0.60	0.27	-0.49	-0.56		1.25	0.56		-5.88
	0.65	0.29		-1.08		1.30	0.58		-6.15
	0.70	0.31		-1.59		1.35	0.60		
	0.75	0.34		-2.10		1.40	0.63		
	0.80	0.36		-2.59		1.45	0.65		
	0.85	0.38		-3.08					

[a] Segmental density (or volume fraction) of the mobile phase in terms of segments per lattice cell. [b] ln k' generated by eq 8 with $\epsilon_{st}/kT = -1.01$ and $\epsilon_{mt}/kT = -0.95$.

Figure 5 are plots of ln k' vs θ_m for three- and four-ring PAH compounds at constant temperature. It is obvious that the three-ring PAHs have less negative slopes compared with the four-ring ones. The four-ring PAH isomers with almost the same contact areas (38.54, 38.29, and 37.65 for benz[a]anthracene, triphenylene, and benzo[c]phenanthrene, respectively) have nearly the same slopes. As can be seen in Figure 5, pyrene should intersect with benzo[c]phenanthrene at sufficiently high mobile phase density.[9]

Putting the experimental parameters ($\theta_s = 0.63$, $\omega = 2.20$, $q = 1.43$, $r = 2.63$) into eq 1, we have

$$\ln (3K) = -0.57ab - 0.44(ac + bc)\frac{\epsilon_{st}}{kT} - abc \ln\left[\frac{1-\theta_m}{1-0.41\theta_m}\right] + (ab + ac + bc)2\frac{\epsilon_{mt}}{kT}\left[\frac{0.59\theta_m}{1-0.41\theta_m}\right] \quad (8)$$

where $abc = V_w$ (scaled volume[9]) and $K = \phi k'$.

Rearranging eq 8, we have

$$\ln k' = -0.57A_{min} - 0.44(ac + bc)\frac{\epsilon_{st}}{kT} - V_w \ln\left[\frac{1-\theta_m}{1-0.41\theta_m}\right] + A_{ef}\frac{\epsilon_{mt}}{kT}\left[\frac{0.59\theta_m}{1-0.41\theta_m}\right] - 5.52 \quad (9)$$

For a particular solute, V_w, A_{ef}, and A_{min}, and $(ac + bc)$ are all fixed; therefore, ϵ_{st} and ϵ_{mt} will be left as the only unknown parameters. Let us take triphenylene as an example. From Table II, we have $V_w = 34.29$, $A_{ef} = 38.29$, $A_{min} = 6.60$, and $ac + bc = 31.69$. Substituting these parameters into eq 9, one obtains

$$\ln k' = -13.94\frac{\epsilon_{st}}{kT} - 34.29 \ln\left[\frac{1-\theta_m}{1-0.41\theta_m}\right] + 38.39\frac{\epsilon_{mt}}{kT}\left[\frac{0.59\theta_m}{1-0.41\theta_m}\right] - 9.28 \quad (10)$$

Using the values of ln k' and mobile phase densities in Table IV, best-fit analysis according to eq 10 yields $\epsilon_{st}/kT = -1.01$ and $\epsilon_{mt}/kT = -0.95$, indicating slightly stronger attractive solute–stationary phase (PAH–liquid crystal) segmental interactions compared to solute–mobile phase (PAH–CO_2) segmental interactions. For all PAH solutes, ϵ_{st} and ϵ_{mt} should be the same at constant temperature (assuming ϵ_{st} and ϵ_{mt} are density independent). Therefore, we can use eq 9 to predict the retention times for other solutes, assuming only that the energetic parameters are known. If the theory does not properly describe solute retention, the retention times generated will not fit the experimental data. Shown in Figure 6 are plots of ln k' vs mobile phase density for four-ring PAH isomers using the theoretical and the experimental values in Table V. The agreement between the theory and the experiment is good. In other words, we would obtain approximately the same interaction energies by solving eq 9 using the retention times and relevant parameters of the different solutes.

It is interesting to note that minima are predicted at *very* high mobile phase densities, i.e., $\rho_m > 1.30$ g/mL (see Table V). Martire and Boehm[16] in their unified theory predicted the possibility of minima in the plots of ln k' vs ρ, *under certain conditions*.

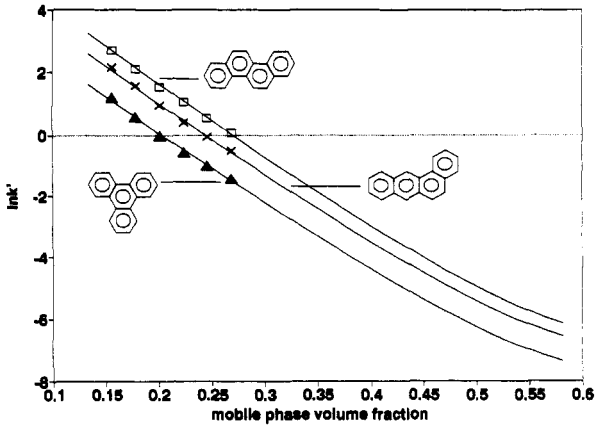

Figure 6. Plots of ln k' vs SF CO_2 mobile phase density for four-ring PAH isomers on the SB–smectic column, as predicted by eq 10. Symbols: experimental data.

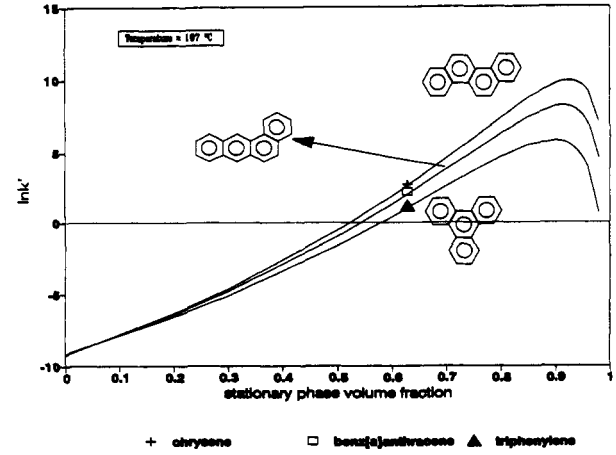

Figure 7. Plots of ln k' vs stationary phase volume fraction (θ_s) for four-ring PAH isomers on the SB–smectic phase at 107 °C and SF CO_2 density of 0.35 g/mL, as predicted by the theory. Symbols: experimental data.

However, as they pointed out, there has been only a mention of the existence of such minima in the SFC literature. For PAH/μ-Bondopak–NH_2/CO_2 systems at 40 °C Christensen[17] observed common minima in retention at P = 250 atm (ρ = 0.88 g/mL) for all PAHs studied.

To conclude this subsection, it is clear that ln k' decreases with increasing mobile phase density in the operational region. The slope of ln k' vs θ_m is governed predominantly by the energetic term in the usual density region. Although the entropic term is not large enough to change the declining tendency of ln k' in this region, it makes the slope less negative and eventually zero. In the very high density region, where the entropic term becomes more important, the highly compressed mobile phase makes the packing of the solute molecules into the mobile phase more difficult and would therefore tend to drive the solute toward the stationary phase, more so when the solute molecule has a larger van der Waals volume. As a consequence, ln k' increases with increasing θ_m in that region. The stationary-phase contribution governs only the intercept, according to our model. Although a minimum in ln k' vs θ_m is predicted, it will be difficult (if not impossible) to attain in practice, since it occurs at such a high mobile phase density.

4.3. Effect of Stationary Phase Parameters. With the mobile phase variables fixed, the sum of the second and last terms in eq 1 will be a constant for a particular solute at constant temperature. Then, eq 1 becomes

$$\ln k' = ab \ln\left[\frac{1-\theta_s}{1-\theta_s(1-1/\omega)}\right] - \left[\frac{2(ac+bc)\epsilon_{st}}{kT}\right]\left[\frac{\theta_s(1/\omega)}{1-\theta_s(1-1/\omega)}\right] + \ln k^\circ \quad (11)$$

where ln k° = the second term in eq 1 + the fourth term − ln 3ϕ is the limiting value when the stationary phase density approaches zero.

The first term in eq 11, which arises from the configurational entropy of the solute in the stationary phase, leads to a decrease in ln k' (or ln K) with increasing stationary phase density (θ_s) for a particular solute. The second term in eq 11, which arises from the stationary phase–solute attractive interactions, leads to an increase in ln k' with increasing θ_s or decreasing T. The overall contributions from the stationary phase should be a combination of the entropic and energetic effects. Figure 7 was constructed using the parameters determined previously (see Figure 6), and by assuming that both the stationary phase and the solute remain fully aligned in the preferred direction over the entire θ_s region (eq 11). The natural logarithm of the capacity factor, ln k', increases with increasing θ_s in the lower stationary phase density region where the energetic term is obviously dominant on an absolute basis, gradually approaches a maximum, then decreases with increasing θ_s in the higher density region where the entropic term becomes dominant. For four-ring PAH isomers at 0.35 g/mL mobile phase density the predicted maxima appear at about 0.95 segment/cell, a value which is hardly accessible. There is only one experimental data point for each solute since only one column was used in this study. Although it is believed that the general trend of ln k' vs θ_s predicted by eq 11 is reasonable, it remains to be experimentally confirmed. It should be noted, however, that a similar trend for ln K vs θ_s (alkyl chain bonding density) in reversed-phase LC has been predicted[3,4] and observed.[18]

4.4. Effect of Temperature. In the preceding paper,[9] we derived and discussed the following expression for the capacity factor (see eqs 82–85 in ref 9):

$$\ln k' = -\Delta H/RT + \Delta S/R - \ln \phi \quad (12)$$

where

$$\Delta H = H^s - H^m = 2(ac+bc)L\epsilon_{st}\left[\frac{\theta_s(1/\omega)}{1-\theta_s(1-1/\omega)}\right] - 2(ab+ac+bc)L\epsilon_{mt}\left[\frac{\theta_m\left(\frac{2}{3q}+\frac{1}{3r}\right)}{1-\theta_m\left(1-\frac{2}{3q}-\frac{1}{3r}\right)}\right] \quad (13)$$

$$\frac{\Delta S}{R} = \frac{S^s}{R} - \frac{S^m}{R} = ab \ln\left[\frac{1-\theta_s}{1-\theta_s(1-1/\omega)}\right] - abc \ln\left[\frac{1-\theta_m}{1-\theta_m\left(1-\frac{2}{3q}-\frac{1}{3r}\right)}\right] - \ln 3 \quad (14)$$

where L is Avogadro's number. Now, with eqs 13 and 14, we can understand, at the molecular level, the physical significance of the enthalpy transfer (ΔH) and the entropy transfer (ΔS) of the solute from the isotropic mobile phase to the anisotropic stationary phase. Equation 13 reveals that the so-called solute enthalpy of transfer is the difference between the energetic term (attractive interactions) for the solute in the mobile phase (H^m) and the energetic term for the solute in the stationary phase (H^s). Equation 14 reveals that the solute entropy of transfer is simply the dif-

(16) Martire, D. E.; Boehm, R. E. *J. Phys. Chem.* **1987**, *91*, 2433.
(17) Christensen, R. G. *J. High Resolut. Chromatogr. Chromatogr. Commun.* **1985**, *8*, 824.
(18) Sentell, K. B.; Dorsey, J. G. *Anal. Chem.* **1989**, *61*, 930.

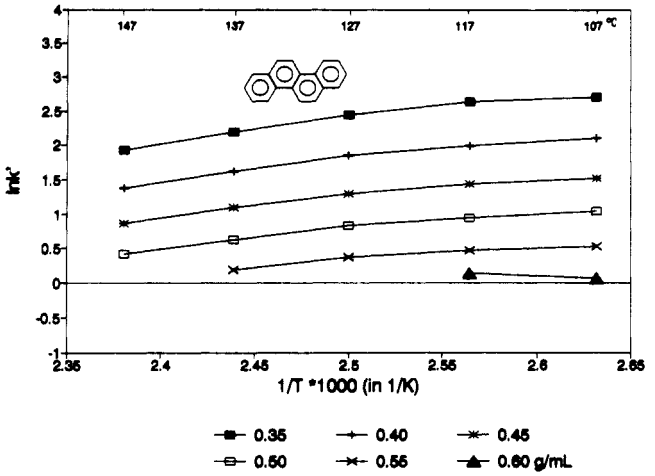

Figure 8. van't Hoff plots for chrysene on the SB–smectic column with SF CO_2 mobile phase at different densities.

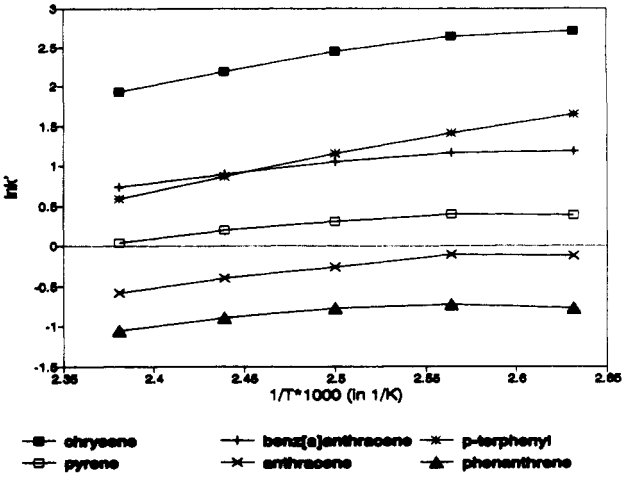

Figure 9. van't Hoff plots for PAH compounds on the SB–smectic column at SF CO_2 density of 0.35 g/mL.

ference between the entropic packing term for the solute in the mobile phase (S^m) and the packing term for the solute in the stationary phase (S^s). Furthermore, knowing the parameters in eqs 13 and 14, we can estimate the values of ΔH and ΔS. For a specific chromatographic system at constant mobile phase density, the van't Hoff plot ($\ln k'$ vs $1/T$) according to eq 12 should give a slope of $-\Delta H/R$ and an intercept of $(\Delta S/R) - \ln \phi$. If ΔH is a constant throughout the temperature region, then the van't Hoff plot should be linear. If ΔH is not a constant, then a curve should be observed. Keep in mind that

$$-\text{slope} = \Delta H/R = (H^s - H^m)/R \qquad (15)$$

where H^s and H^m are always negative since both ϵ_{st} and ϵ_{mt} are negative.

The following is a summary of the trends predicted by eqs 12 and 13: (a) the van't Hoff plot should be linear provided that ΔH is constant; (b) the slope should be positive ($\Delta H \leq 0$) in most chromatographic systems (especially in GC and SFC), because the mobile phase density (θ_m) is usually much lower than the stationary phase density (θ_s) and $|\epsilon_{st}| \geq |\epsilon_{mt}|$ in most chromatographic systems; consequently, $\Delta H \leq 0$, and slope ≥ 0; (c) under the same conditions, the solute with a larger ratio of contact area with the stationary phase to the contact area with the mobile phase should have a larger slope; (d) the slope should decrease with increasing mobile phase density since a higher θ_m would make H^m more negative. Also, if a phase transition is involved in the operational temperature range, we would expect a discontinuity or a change in the slope.

Figure 8 shows plots of the natural logarithm of the capacity factor ($\ln k'$) vs the reciprocal temperature (van't Hoff plots) for chrysene on the SB–smectic column. There is no break or obviously sharp change in the slope of $\ln k'$ vs $1/T$ in the temperature range although the lines are clearly not linear. The nonlinearity may be caused by the temperature dependence of the orientational order parameter and the density of the stationary phase. The signs of the slopes are positive at all mobile phase densities with the possible exception of the one at the highest density (0.60 g/mL); therefore, our experimental results are in agreement with predictions a, b, and d. Figure 9 illustrates plots of $\ln k'$ vs $1/T$ for PAH compounds with different numbers of rings at a mobile phase density of 0.35 g/mL. As has been observed by Lee et al.,[13] we also find a crossover (triphenylene and *p*-terphenyl) phenomenon. Triphenylene and *p*-terphenyl have almost the same contact area with the mobile phase (38.29 and 38.33, respectively), but *p*-terphenyl has a relatively larger contact area with the stationary phase (33.53) compared with triphenylene (31.69 Å^2). Therefore, we have

$$H^m_{\text{triphenylene}} \approx H^m_{p\text{-terphenyl}}$$

but

$$H^s_{\text{triphenylene}} > H^s_{p\text{-terphenyl}}$$

hence

$$\Delta H_{\text{triphenylene}} > \Delta H_{p\text{-terphenyl}}$$

Thus, the slope for triphenylene should be smaller than the slope for *p*-terphenyl. Similarly, chrysene (anthracene) has a larger slope than triphenylene (phenanthrene) because it has a *relatively* larger contact area with the stationary phase. Prediction c is thus confirmed.

5. Conclusion

Our experimental study has shown that the smectic liquid-crystalline phase has excellent shape selectivity for PAH compounds. The blocklike solutes (PAHs) tend to penetrate more readily into the brushlike stationary phase with their plane of minimum area perpendicular to the preferred direction of the rodlike side chains, and in so doing they also interact with the stationary phase more efficiently. The SFC experimental data have been used for testing the molecular theory of chromatography presented in the preceding article.[9] The agreement between the theoretical predictions and the experimental results is encouraging.

Finally, it should again be noted that the analysis and interpretation of the data have been based on a model which neglects the effects of swelling of the stationary-phase polymer by CO_2[1] and incomplete alignment of the polymer side chains. These issues will be addressed in a subsequent study.

Acknowledgment. This material is based upon work supported by the National Science Foundation under Grant CHE-8902735.